

Experimental Communication

Cite

Karavyraki M, Gnaiger E, Porter RK (2022) A comparison of bioenergetics in human tongue pre-cancerous dysplastic oral keratinocytes and squamous cancer cells. MitoFit Preprints 2022.22.

<https://doi.org/10.26124/mitofit:2022-0022>

Author contributions

EG and RP conceived and planned the experiments. RP supervised the project. MK performed the experiments. All authors discussed the results and contributed to the final manuscript.

Conflicts of interest

EG is founder and CEO of Oroboros Instruments.

Received 2022-06-02

Accepted 2022-06-02

Online 2022-06-02



Data availability

All data will be available.

Keywords

oral squamous cancer cells;
mitochondria;
interleukin 6;
dysplastic oral keratinocytes;
oxygen consumption

A comparison of bioenergetics in human tongue pre-cancerous dysplastic oral keratinocytes and squamous cancer cells

Marilena Karavyraki¹,  Erich Gnaiger²,
 Richard K Porter¹

1 School of Biochemistry, Trinity Biomedical Science Institute, Trinity College Dublin, Ireland

2 Oroboros Instruments, Innsbruck, Austria

* Corresponding author: rkporter@tcd.ie

Summary

In an endeavour to understand the metabolic phenotype behind oral squamous cell carcinomas, we characterised the bioenergetic profile of a human tongue derived cancer cell line (SCC-4 cells) and compared this profile to a pre-cancerous dysplastic oral keratinocyte (DOK) cell line also derived from human tongue. The human SCC-4 cancer cells had greater mitochondrial density but lower mitochondrial O₂ flow per cell than DOK cells. The lower oxygen consumption rate in SCC-4 cells can be partially explained by lower NADH-related enzymatic activity and lower mitochondrial Complex I activity when compared to pre-cancerous DOK cells. In addition, SCC-4 cells have greater extracellular acidification rate (an index of glycolytic flux) when compared to DOK cells. In addition, treatment with recombinant human IL-6 (rhIL-6), known to drive anoikis resistance in SCC-4 cells but not DOK cells, impairs oxygen consumption in SCC-4 but not DOK cells, without affecting mitochondrial density. We conclude that SCC-4 cells have a less oxidative phenotype compared to DOK cells and that IL-6 attenuates mitochondrial function in SCC-4 cells while increasing glycolytic flux.

1. Introduction

Oral squamous cell carcinoma (OSCC) is the sixth most common cancer worldwide (Blatt et al 2017). The majority of the oral cancer cases appear on the ventral-lateral edge of the tongue (40 %), floor of the mouth (30 %) and lower lip (Yellowitz et al 2000; Bagan et al 2010) and most commonly metastasizes to lymph nodes (Okura et al 2009). Surgical

removal of the tumour, combined with radiation and chemotherapy, are the usual treatment regimens against OSCC, but they are only moderately successful (Moore et al 2000; Dong et al 2015). Thus, there is justification in seeking novel therapeutic targets for the treatment of oral cancer. *In vitro* models used to investigate OSCC include culturing squamous cell carcinoma-4 (SCC-4) cells, which were originally established from the tongue of a 55-year-old male (Rheinwald, Beckett 1981). In regard to oral cancer, IL-6 production has been correlated with poor prognosis in oral carcinomas (Jinno et al 2015). In relation to SCC-4 cells in particular, it been demonstrated that SCC-4 cells have membrane bound IL-6 receptor (IL-6R/gp180) and that IL-6 drives *anoikis* resistance in these cells in an autocrine fashion and on addition of rhIL-6 (Karavyraki, Porter 2022). Other studies have also demonstrated that IL-6 enhances migration of SCC-4 cells (Chuang et al 2014), proliferation (Chen et al 2012) and mediates osteoclastogenesis in SCC-4 cells (Tang et al 2008). In an endeavour, to understand the metabolic phenotype behind metastasis from oral squamous cell carcinomas, we characterised the bioenergetic profile of a human tongue derived cancer cell line (SCC-4 cells) (Rheinwald, Beckett 1981) and compared this profile to a pre-cancerous dysplastic oral keratinocyte (DOK) cell line also derived from human tongue. According to the controversial Warburg effect, a less oxidative metabolic profile might be expected in the SCC-4 cancer cells, compared to the dysplastic cells (DOK) (Warburg, 1956). In addition, we anticipated seeing a further decrease in SCC-4 cancer cell oxidative metabolism again commensurate with driving a pro-cancer phenotype (Tang et al 2008; Chuang et al 2014; Karavyraki, Porter 2022).

2. Methods

2.1. DOK and SCC-4 cell lines

Dysplastic oral keratinocyte (DOK) cells were originally isolated from a piece of dorsal tongue of a 57-year-old male. DOK cells [cat# ECACC 94122104] are characterized as Caucasian derived epithelial adherent tongue dysplastic cells. Squamous cell carcinoma (SCC-4) cells were originally established from the tongue of a 55-year-old male [SCC-4 cat# ECACC 89062002]. Mycoplasma-free cells were grown in cell culture flasks in Dulbecco's Modified Eagle's Medium GlutaMAX cell culture medium (Gibco) supplemented with 5 µg/mL hydrocortisone, 20 % (v/v) Foetal Bovine Serum (FBS) and penicillin-streptomycin (50 U/mL and 50 µg/mL) (Gibco). Cells were grown at 37 °C in humidified environment containing 95 % O₂ and 5 % CO₂. DOK and SCC-4 cells were passaged at least twice weekly depending on their levels of confluency (75-80 %) and were purchased from the European Centre of Authenticated Cell Culture. In terms of validity of comparability, all cells used in this study originated from the human buccal cavity and represent primary (PGK), pre-cancerous (DOK) and cancerous (SCC-4) cells, with the latter two being from the same tissue (tongue).

2.2. Oxygen consumption rate and extracellular acidification analysis using the Seahorse XF Analyzer

The Seahorse XF Analyzer (Agilent, Santa Clara, US) provides multi-well plate analysis of two processes in real time, namely oxygen consumption rate as an indicator of cell respiration and extracellular acidification rate largely dependent on glycolytic processes (Gu et al 2021). Cellular oxygen consumption causes changes in the concentration of dissolved dioxygen (O₂) in 'transient microchambers' as determined by

solid-state fluorescent probes. Additions are injected pneumatically, limited to four sequential injections per well. The medium used for Seahorse experiments was XF Assay Medium supplemented with the desired concentration of glucose.

2.3. High-resolution respirometry by Oroboros O2k

High-resolution respirometry by Oroboros Oxygraph-2k (O2k) *Coupling Control Protocol* (CCP) induces different coupling control states at constant substrate supply (Gnaiger 2020). The medium used in experiments was MiR05-Kit (0.5 mM EGTA, 3 mM MgCl₂·6H₂O, 60 mM lactobionic acid, 20 mM taurine, 10 mM KH₂PO₄, 20 mM HEPES, 110 mM D-sucrose, and 0.1 % (w/v) fatty-acid free BSA, pH 7.1 at 30 °C), which does not contain mitochondrial fuel substrates.

2.4. Biolog™ Mitoplate S-1 microplate analysis

Biolog™ Mitoplate S-1 Microplates were used to screen various mitochondrial substrates that result in electron transfer ET activity. Substrates, coated on the bottom of the Mitoplate S-1, were dissolved using 30 µL per well of the assay mix, which is comprised of 2x Biolog MAS media, 6x Redox Dye MC, 24x saponin and sterile H₂O. Microplates were incubated in a sealed plastic bag for 1 hour prior to cell seeding at 37 °C to prevent evaporation of the medium and safeguard against atmospheric CO₂ of the incubator. Upon incubation, cells were trypsinised, centrifuged at 300 *g* for 5 min and seeded at a final cell concentration of 10⁶ x/mL in 30 µL of 1x Biolog MAS (30 000 cells per well). The plate was loaded in the OmniLog™ set at 37 °C to record Redox Dye decrease over time.

2.5. Citrate synthase activity assay

Citrate synthase enzyme activity was measured spectrophotometrically by a colorimetric coupled reaction, originally described by Srere (1969). The citrate synthase activity is determined by monitoring the rate of production of thionitrobenzoic acid (TNB) at a wavelength of 412 nm. Cells were subjected to three freeze thaw cycles in liquid nitrogen immediately prior to being assayed. Cell lysates were incubated at 30 °C in a 1mL cuvette with Tris Buffer (0.2 M, pH 8.1), and the following reaction components were added in the corresponding concentrations; 5,5'- dithiobis- (2-nitrobenzoic acid) (DTNB) (0.1 mM), acetyl coenzyme A (0.3 mM) and Triton X (0.1 %). Freshly prepared oxaloacetate (0.5 mM) was added to initiate the reaction and an increase in the absorbance was monitored for 3 min. Our laboratory has previously demonstrated that citrate synthase activity gives an equivalent index of mitochondrial density when compared to immunoblotting for the mitochondrial outer membrane protein VDAC and the mitochondrial inner membrane protein cytochrome *c* oxidase subunit 4 (Geoghegan et al 2017a).

2.6. NADH ubiquinone oxidoreductase (Complex I) activity assay

The activity of NADH-ubiquinone oxidoreductase (Complex I) was determined by monitoring the oxidation of NADH at 340 nm (Spinazzi et al 2012). Cell lysates were incubated at 30 °C in a 1 mL cuvette with potassium phosphate buffer (25 mM, pH 7.5), fatty acid free bovine serum albumin (BSA) (3 mg·mL⁻¹), KCN (0.3 mM), and NADH (0.1 mM). A blank rate was measured for 2 min before ubiquinone₁ (60 µM) was added to the cuvette to start the reaction and a decrease in absorbance was monitored for 3 min.

Afterwards, rotenone (10 μM) was added to measure the rotenone-resistant activity and the rate was monitored for another 2 min. The specific Complex I activity is calculated as the rotenone-sensitive activity determined by subtracting the rotenone-resistant activity (with rotenone) from the total activity (without rotenone).

2.7. Protein determination using the bicinchoninic acid (BCA) assay

Quantification of protein concentrations in cell lysates was carried out using the Bicinchoninic Acid (BCA) assay as described by Smith et al (1985).

2.7. Statistical analysis

Statistical analyses were performed using the computer based mathematical package Graph Pad Prism 8.0 software. All results were expressed as mean \pm standard error of the mean for N number of independent experimental replicas (mean \pm sem(N)) performed with at least three technical repeats ($n \geq 3$) For comparisons of two groups, data were analyzed using a two-tailed unpaired student's *t-test*, while for comparisons of more than two groups, data were analyzed using one-way or two-way ANOVA followed by Tukey's or Sidak's or Bonferroni's multiple comparison tests were performed. Absolute *p*-values are given.

3. Results

3.1. Comparison of cellular metabolic/bioenergetic function in dysplastic oral keratinocytes (DOK) cells and immortal squamous cell carcinoma 4 (SCC-4) cells in suspension using the Seahorse Flux Analyzer

Significantly different total ROUTINE respiration rates R'_{tot} were measured as O_2 flow per cell I_{O_2} for DOK and SCC-4 cells at 112 ± 3 (6) and 87 ± 6 (6) $\text{amol O}_2 \cdot \text{s}^{-1} \cdot \text{x}^{-1}$, respectively, where x is the single cell. Rotenone and antimycin A (1 μM and 3 μM final concentration, respectively) were used to determine the oxygen consumption not due to mitochondrial electron transfer (residual oxygen consumption R_{ox}) which was 18.3 ± 1.8 (6) and 21.1 ± 4.8 (6) $\text{amol O}_2 \cdot \text{s}^{-1} \cdot \text{x}^{-1}$, for DOK and SCC-4, respectively. ROUTINE respiration R was determined by subtracting R_{ox} from R'_{tot} and was significantly different at 93.5 ± 3.1 (6) and 65.6 ± 4.9 (6) $\text{amol O}_2 \cdot \text{s}^{-1} \cdot \text{x}^{-1}$ for DOK and SCC-4 cells, respectively (Figure 1a).

As demonstrated in Figure 1a, DOK cells demonstrated significantly greater mitochondrial oxygen consumption OCR when compared to SCC-4 cells. In our endeavour to explain this differential oxygen consumption rate, we looked for differences in mitochondrial density. Cell lysates were used for citrate synthase activity measurements and activity was expressed per unit protein concentration. Interestingly and surprisingly, there was significantly higher mitochondrial density, as determined by citrate synthase activity, in SCC-4 cells when compared to DOK cells: 36.2 ± 1.7 (12) versus 15.2 ± 1.9 (9) $\text{nmol} \cdot \text{min}^{-1} \cdot \text{mg}^{-1}$ protein (mean \pm SEM (N), respectively (Figure 1b).

The extracellular acidification rates (ECAR) under ROUTINE conditions, for DOK and SCC-4 cells were 11 ± 1 (6) and 25 ± 1 (6) $\text{npH} \cdot \text{s}^{-1} \cdot \text{x}^{-1}$, respectively, (Figure 1c). The extracellular acidification rate, an indirect indicator of glycolytic flux, was significantly higher in SCC-4 cells compared to DOK cells.

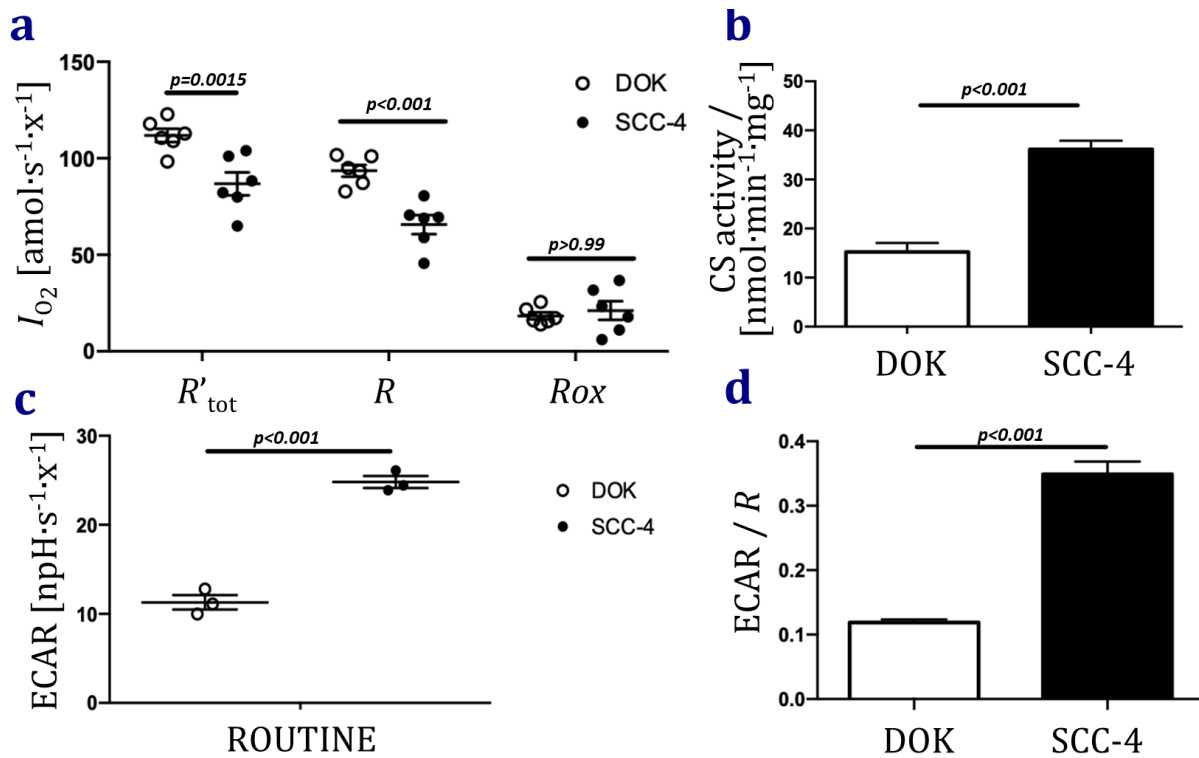


Figure 1. Cellular bioenergetics in dysplastic oral keratinocytes DOK and squamous cell cancer cells (SCC-4 cells) in the Seahorse Flux Analyzer. (a) Total ROUTINE R'_{tot} and ROUTINE respiration R (corrected for R_{ox}), and residual oxygen consumption R_{ox} ; **(b)** citrate synthase CS activity, **(c)** extracellular acidification rate, and **(d)** ECAR/ R ratio, in DOK and SCC-4 cells. Values are expressed as mean \pm SEM (N).

The ratio of extracellular acidification rate to mitochondrial oxygen consumption rates (ECAR/ R) was calculated by dividing the ECAR to R and highlights the fact that SCC-4 cells (0.35 ± 0.02 (6)) are significantly more glycolytic than DOK cells (0.12 ± 0.01 (6)) (mean \pm SEM (N); Figure 1d). Since ECAR is expressed on a logarithmic scale, this ratio cannot be interpreted as a metabolic flux ratio.

3.2. Comparison of electron transport systems in dysplastic oral keratinocytes (DOK) cells and immortal squamous cell carcinoma 4 (SCC-4) cells in suspension using the Oroboros O2k

The metabolic/bioenergetic function in dysplastic oral keratinocytes (DOK) cells and immortal squamous cell carcinoma 4 (SCC-4) cells, were compared using the Oroboros High-Resolution Respirometer O2k (Figure 2). This work used the ‘Coupling Control Protocol’ as suggested by the manufacturer, Oroboros Instruments. Figure 2a shows representative traces of respiration comparing the oxygen flow between the DOK and SCC-4 cell lines. After pyruvate addition, ROUTINE respiration slightly increased in both cell lines but remained statistically insignificant from each other. In the presence of oligomycin which inhibits ATP synthesis, LEAK respiration in both DOK and SCC-4 cells was decreased, as expected. After uncoupler (CCCP) titration in the presence of oligomycin, ET capacity in SCC-4 cells was significantly decreased when compared to DOK cells. The collated data for 6 of these experiments is given in Figure 2b. O_2 flow per cell [$\text{amol } O_2\cdot\text{s}^{-1}\cdot\text{x}^{-1}$] was significantly higher in living DOK cells in the presence of pyruvate (68.4 ± 5.3 (6)), glucose (169.5 ± 15 (6)) and malate (180.2 ± 13.2 (6)) when compared to

living SCC-4 cells (54.2 ± 5 , 102.1 ± 9 , 104.2 ± 7.4 (7), respectively). However, after cell permeabilization with digitonin, no significant differential rates were observed in the presence of succinate (DOK: 80.7 ± 16.1 (6); SCC-4: 84.1 ± 5.6 (7)).

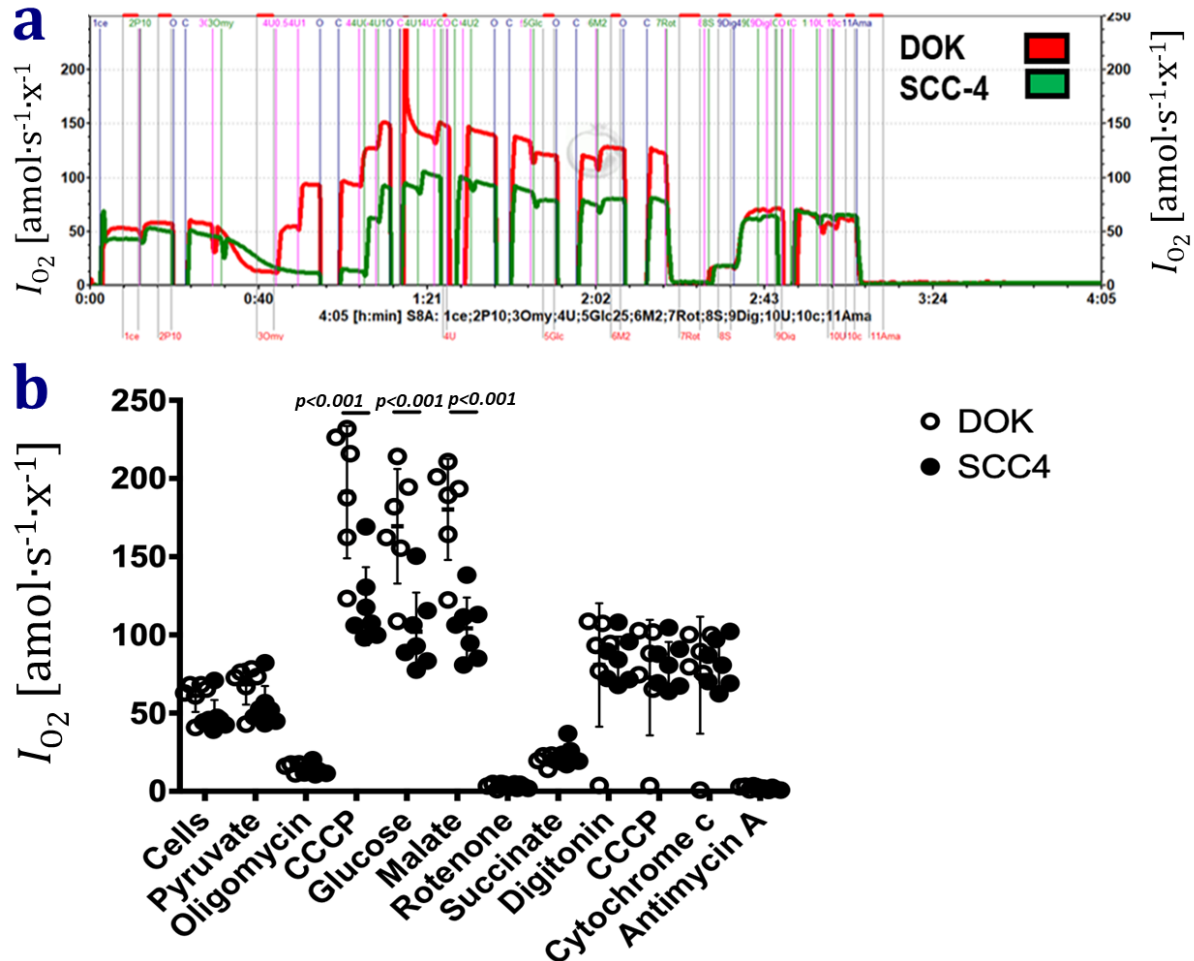


Figure 2. Oroboros O2k analysis of DOK (red) vs SCC-4 (green) using the coupling control protocol. (a) Representative plots of oxygen flow I_{O_2} in (red) DOK and (green) SCC-4 cells. Key: 1ce, cells-no substrate; 2P10, 10 mM pyruvate; 3U, 2.5 μM CCCP; 4Glc, 25 mM glucose; 5M, 2 mM malate; 6Rot, 5 μM rotenone; 7S, 10 mM succinate; 8Dig, 0.0041 $\mu\text{M} \times 2$ digitonin; 9U, 0.5 μM CCCP; 9c, 10 μM cytochrome c; 10Ama, 2.5 μM antimycin A. **(b)** Collated data demonstrates that I_{O_2} in the presence of pyruvate, glucose and malate was higher in living DOK cells compared to SCC-4 cells. Glucose exerted a small inhibitory Crabtree effect. Results represent six and seven experiments performed in triplicate (mean \pm SEM (n)), p -values where shown indicate significance (two-way ANOVA with Bonferroni multiple comparison post *hoc* test).

3.3. A comparison of enzymatic metabolic/bioenergetic function in dysplastic oral keratinocytes (DOK) cells and immortal squamous cell carcinoma 4 (SCC-4) cells using the BiologTM Mitoplate assay and NADH dehydrogenase assay

The mitochondrial metabolic phenotype of DOK and SCC-4 cells was investigated further using the phenotypic Mitoplate S-1 assay, to determine whether there were any differences in their mitochondrial enzyme activities (Figure 3). DOK and SCC-4 were permeabilised with saponin so the substrates in the plate were immediately available to

be metabolised. The key observation was that DOK cells appeared to have higher TCA cycle enzyme activities compared to SCC-4 cells, as indicated by significantly greater metabolism of α -keto-glutaric acid ($p=0.015$), succinic acid ($p=0.018$) and L-malic acid ($p=0.016$), whereas SCC4 cells have greater glutamate and glutamine catabolism ($p=0.016$). Furthermore, there was a 2-fold ($p<0.01$) greater activity of mitochondrial NADH dehydrogenase (Complex I) associated with DOK cells compared to SCC4 cells (Figure 3b).

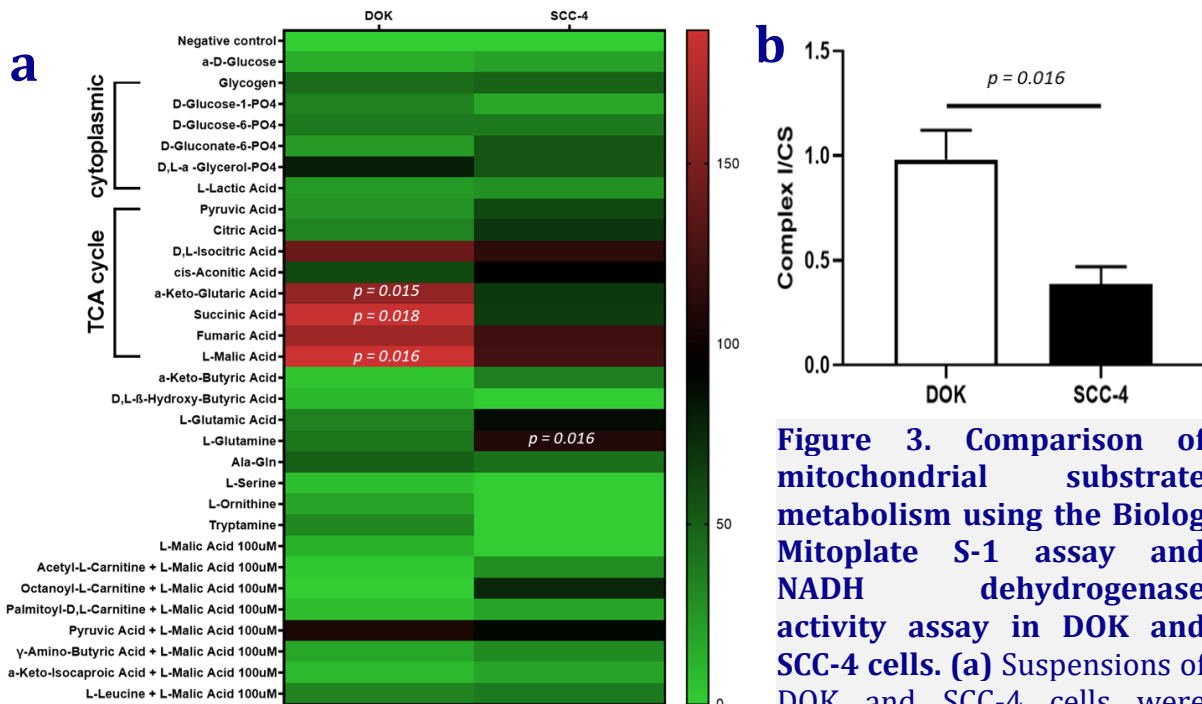


Figure 3. Comparison of mitochondrial substrate metabolism using the Biolog Mitoplate S-1 assay and NADH dehydrogenase activity assay in DOK and SCC-4 cells. (a) Suspensions of DOK and SCC-4 cells were

inoculated into the Mitoplate S-1 plates (Biolog, Hayward, CA) which contained 31 substrates. Negative controls had no substrate in the well. Wells containing α -D-glucose served as positive controls. Thresholds were set to disregard small and insignificant changes, and all wells that exceeded this threshold are marked to denote differentially metabolized substrates for each cell line, which are described in the text. Heat map presents mitochondrial substrate utilization patterns of DOK and SCC-4 cells under non-starved conditions. Phenotypes that are lost are coloured green and phenotypes that are gained are coloured red; the exact relative values are given by a corresponding colour as indicated on the colour scales. Heat map shows collated data from 4 independent experiments. Statistical analysis performed with Holm-Sidak method. **(b)** NADH dehydrogenase activity was determined using the method of Spinazzi et al (2012). Statistical analysis was performed using ANOVA for 3 independent experiments performed in triplicate.

3.4. Effect of rhIL-6 on metabolic/bioenergetic function and respiratory profile of SCC-4 cells in the Seahorse Flux Analyser

In light of the fact that SCC-4 cells express the IL-6/gp180-linked receptor, whereas DOK cells do not (Karavyraki, Porter 2022), we investigated the effect of added IL-6 on bioenergetic function in these cells. Thus, recombinant human (rh) IL-6 (rhIL-6), was added to cells for a period of 24 h (Figure 4), at a time and concentration known to be effective in promoting *anoikis* resistance in SCC-4 cells (Karavyraki, Porter 2022). Figure 4a demonstrates that protein-specific O_2 flux [$\mu\text{mol } O_2 \cdot \text{s}^{-1} \cdot \text{mg}^{-1}$] (mean \pm SEM (N)) of DOK

cells was not significantly affected by addition of rhIL-6 (control value of 4 ± 0.2 (3) versus 3.7 ± 0.2 (3) for rhIL-6 treated cells). However, ROUTINE respiration decreased significantly ($p \leq 0.001$) in SCC-4 cells following treatment with rhIL-6 from 3.6 ± 0.2 (3) to 1.6 ± 0 (3). This decrease in O_2 flux cannot be accounted for by any change in mitochondrial density as citrate synthase levels were equivalent in untreated SCC-4 cells and SCC-4 cells treated with rhIL-6 (Figure 4b). In a mirror image of what was observed for cellular oxygen consumption, extracellular protein-specific acidification rates in SCC-4 cells were increased ($p \leq 0.001$) when rhIL-6 was added from 1.4 ± 0.01 (3) to 2.05 ± 0.01 (3) $\text{mpH}\cdot\text{s}^{-1}\cdot\text{mg}^{-1}$ (mean \pm SEM (N)) (Figure 4c), whereas there was no significant effect of rhIL-6 treatment of DOK cells (1 ± 0.1 (3) $\text{mpH}\cdot\text{s}^{-1}\cdot\text{mg}^{-1}$ for the control group versus 1.2 ± 0.1 (3) $\text{mpH}\cdot\text{s}^{-1}\cdot\text{mg}^{-1}$ for the rhIL-6 treated DOK cells). A secondary plot of the ECAR/R ratio for DOK and SCC-4 cells accentuates the significant effect of rhIL-6 on ECAR/R ratio for SCC-4 cells, with no significant effect of rhIL-6 on ECAR/R ratio in DOK cells (Figure 4d).

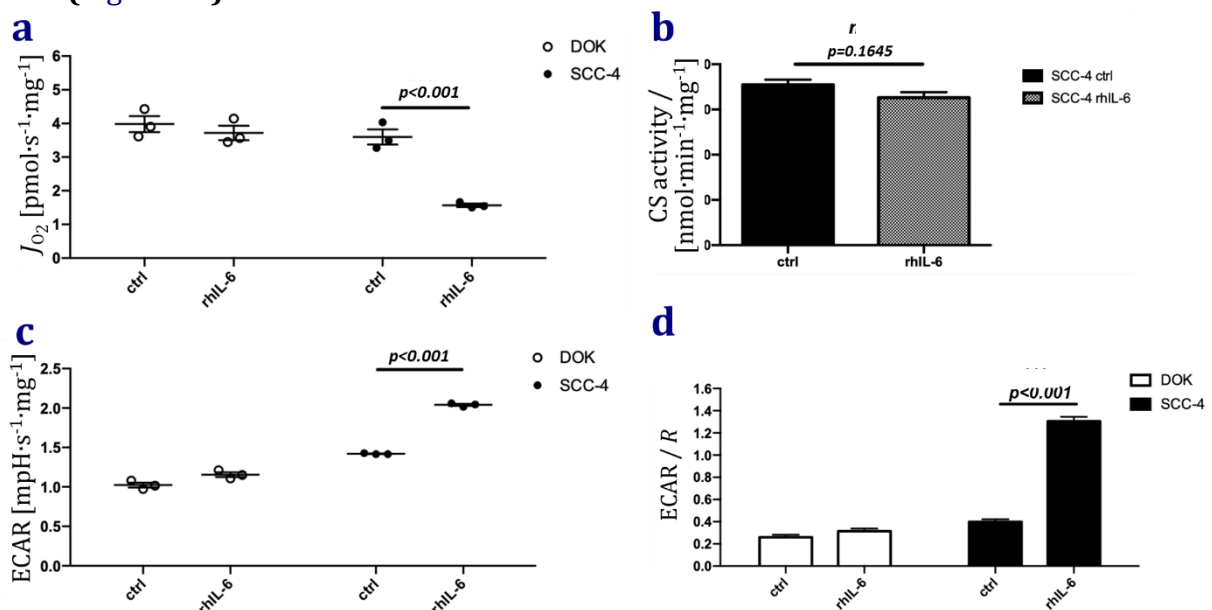


Figure 4. Effect of rhIL-6 on O_2 flux in DOK and SCC-4 cells. (a) Cellular oxygen flux per mg protein, **(b)** citrate synthase activity, an index of mitochondrial density, **(c)** cellular ECAR in DOK and SCC-4 cells treated with or without rhIL-6, and **(d)** ECAR/R ratio for DOK and SCC-4 cells treated with or without rhIL-6.

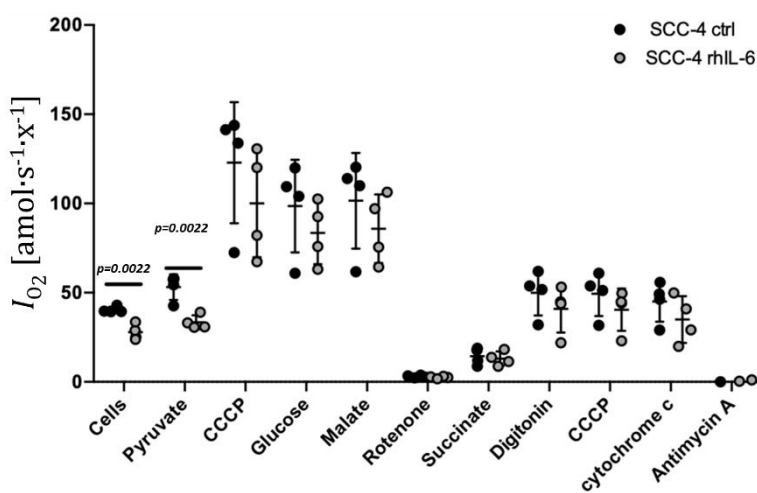


Figure 5. O_2 flow in SCC-4 untreated and treated with rhIL-6 in a coupling control protocol (O_2k). Decreased I_{O_2} (mean \pm SEM; $N=4$) in living SCC-4 cells treated with 30 ng/mL rhIL-6 for 24 h compared to non-treated controls, in the absence of substrate (Cells, 1ce) and presence of 10 mM pyruvate (Pyruvate, 2P10). Two-way ANOVA with Bonferroni multiple comparison post-test.

3.5. Effect of rhIL-6 on metabolic/bioenergetic function and respiratory profile of SCC-4 cells in suspension using the Oroboros High-Resolution Respirometer

To explore the site of inhibition upon rhIL-6 treatment, we again employed the 'Coupling Control Protocol' with the Oroboros O2k. SCC-4 cells were seeded, following treatment with 30 ng/mL rhIL-6 or left untreated (control) for 24 hours. The collated data for the experiments are given in Figure 5. O₂ flow in living untreated SCC-4 cells was significantly ($p = 0.0022$) higher than in SCC-4 treated with rhIL-6, confirming the data in Figure 4. Following pyruvate addition, O₂ flow was again significantly higher ($p = 0.0022$) in living untreated SCC-4 cells compared to SCC-4 cells treated with rhIL-6. No significant differences in O₂ flow were observed, between untreated and rhIL-6 treated SCC-4 cells, after subsequent addition of uncoupler CCCP, glucose, malate, rotenone, succinate, digitonin, more uncoupler or cytochrome *c*. Subsequent addition of antimycin A inhibited mitochondrial oxygen consumption as expected.

4. Discussion

The bioenergetic profiles of human tongue dysplastic oral keratinocytes (DOK) and squamous cell carcinoma (SCC-4) cells were compared. Based on Warburg's (1927) *ex vivo* observations, one might have expected to observe little or no oxidative metabolism and a higher relative glycolytic flux in cancerous SCC-4 cells compared to pre-cancerous DOK cells. It was observed that both DOK and SCC-4 cells have significant mitochondrial oxygen consumption indicating that the mitochondria are active and performing oxidative phosphorylation. Indeed, the cellular and mitochondrial oxygen consumption rates of pre-cancerous DOK cells was ~1.4-fold those of cancerous SCC-4 cells. Thus, in the context of Warburg's observation, it is clear there is no absolute mitochondrial dysfunction in the cancerous SCC-4 but clearly there is a lower oxidative metabolism in SCC-4 cells compared to the pre-cancerous DOK cells.

In an attempt to explain the higher mitochondrial oxygen consumption in DOK cells compared to SCC-4 cells, we measured mitochondrial density, as indexed by citrate synthase activity. Surprisingly, SCC-4 cells had significantly higher (~2.3-fold) mitochondrial density when compared to DOK cells. Thus, if cellular O₂ flux was expressed per unit mass of mitochondria, there was a ~3-fold lower oxygen consumption rate in SCC-4 cells compared to DOK cells. Taking into account the mitochondrial oxygen consumption rate data alone or in combination with mitochondrial density, the data would suggest that there is either (1) some suppression or dysfunction of mitochondrial function in SCC-4 cells compared to DOK cells or (2) that substrate supply to mitochondria in SCC-4 cells is decreased compared to DOK cells.

It was also observed that there was greater (~ 2.3-fold) extracellular acidification (ECAR) in SCC-4 cells compared to DOK cells. ECAR is an index of glycolytic flux due to lactic acid production and release from cells resulting in acidification of the medium. This greater glycolytic flux in SCC-4 cells would be consistent with the aforementioned sub-optimal mitochondrial activity in those cells (compared to DOK cells) and again would be characteristic of cancer tissue (Warburg, 1957) and cancer cells (Hsu et al 2016).

We could find no other published data reporting mitochondrial oxygen consumption rates for DOK cells, but for SCC-4 cells, oxygen consumption rate and ECAR in this study compare well with published data (Duicu et al 2018; Guo et al 2020). Furthermore, the

observation that there was significant mitochondrial oxygen consumption in SCC-4 cancer cells is not unusual in that many laboratories, including our own, demonstrated significant oxidative phosphorylation occurring in various cancer cell lines such as non-small lung cancer cells, mesothelioma cells (Geoghegan et al 2017a), neuroblastoma cells (Geoghegan et al 2017b), triple negative breast cancer cells (O'Neill et al 2019), and prostate cancer cells and tissue (Schöpf et al 2020; Bastos Sant'Anna Silva et al 2021).

Endeavours to understand why mitochondria in SCC-4 cells were operating sub-optimally, compared to those in DOK cells, led to detailed bioenergetic analysis of cellular bioenergetic function. NADH-linked respiratory pathway capacity and mitochondrial Complex I activity were higher in DOK cells compared to SCC-4 cells. This observation is again consistent with aforementioned higher oxygen consumption rates observed in DOK cells compared to SCC-4 cells. Furthermore, the Biolog™ Microarray data compliments that for the coupling control protocol in that DOK cells have higher NADH-related enzyme activities compared to SCC-4 cells. However, it should be pointed out that there is significant oxidative metabolism occurring in SCC4 cells with approximately two-thirds of ATP coming from oxidative phosphorylation, as estimated from respiratory and ECAR fluxes.

Finally, in light of the fact that added rhIL-6 has been demonstrated to enhance *anoikis resistance* in SCC-4 cells (Karavyraki, Porter 2022), it was a logical step to determine whether added rhIL-6 could affect bioenergetic function in these cells. Added rhIL-6 significantly decreased oxygen consumption rates by half and significantly increased extracellular acidification rates (~3-fold) in SCC-4 cells. This decrease in oxygen consumption on addition of rhIL-6 was not due to differences in mitochondrial density and persisted when pyruvate was added to living cells respiring in MiRO5, indicating that rhIL-6 affected (1) substrate supply to mitochondria or (2) attenuated mitochondrial function. It is interesting to note IL-6 has been demonstrated to reduce mitochondrial oxygen consumption in mouse myotubes (Abid et al 2020) but has no effect on mitochondrial consumption in rat hepatocytes (Berthiaume et al 2003). Overall, in this instance, it appears that IL-6 is driving a more cancerous metabolic phenotype in these already cancerous SCC-4 cells.

Abbreviations

CCCP	carbonyl cyanide m-chlorophenyl hydrazone	J_{O_2}	O ₂ flux per cellular protein mass
DOK	dysplastic oral keratinocytes	I_{O_2}	O ₂ flow per cell
ECAR	extracellular acidification rate	OSCC	oral squamous cell cancer
FBS	foetal bovine serum	SCC	squamous cancer cells
IL-6	interleukin-6		

Acknowledgements

Marie Curie Grant TRACT 721906 H2020-MCSA-ITN 2016; COST Action CA15203 MitoEAGLE (2016-2021). We thank Rafael Moreno-Sanchez for a constructive review of our manuscript.

References

- Abid H, Ryan ZC, Delmotte P, Sieck GC, Lanza IR (2020) Extramyocellular interleukin-6 influences skeletal muscle mitochondrial physiology through canonical JAK/STAT signaling pathways. <https://doi.org/10.1096/fj.202000965RR>
- Bagan J, Sarrion G, Jimenez Y (2010) Oral cancer: clinical features. <https://doi.org/10.1016/j.oraloncology.2010.03.009>
- Bastos Sant'Anna Silva AC, Perez Valencia JA, Sciacovelli M, Lalou C, Sarlak S, Tronci L, Nikitopoulou E, Meszaros AT, Frezza C, Rossignol R, Gnaiger E, Klocker H (2021) Succinate anaplerosis has an oncogenic potential in prostate cancer cells. <https://doi.org/doi:10.3390/cancers13071727>
- Berthiaume F, MacDonald AD, Kang, YH, Yarmush ML (2003) Control analysis of mitochondrial metabolism in intact hepatocytes: effect of interleukin-1 β and interleukin-6. [https://doi.org/10.1016/s1096-7176\(03\)00010-7](https://doi.org/10.1016/s1096-7176(03)00010-7)
- Blatt S, Krüger M, Ziebart T, Sagheb K, Schiegnitz E, Goetze E, Al-Nawas B, Pabst AM (2017) Biomarkers in diagnosis and therapy of oral squamous cell carcinoma: A review of the literature. <https://doi.org/10.1016/j.jcms.2017.01.033>
- Chang SE, Foster S, Betts D, Marnock WE (1992) DOK, a cell line established from human dysplastic oral mucosa, shows a partially transformed non-malignant phenotype. <https://doi.org/10.1002/ijc.2910520612>
- Chen M-F, Wang W-H, Lin P-Y, Lee K-D, Chen W-C (2012) Significance of the TGF- β 1/IL-6 axis in oral cancer. <https://doi.org/10.1042/CS20110434>
- Chuang J-Y, Huang Y-L, Yen W-L, Chiang I-P, Tsai M-H, Tang C-H (2014) Syk/JNK/AP-1 Signaling pathway mediates interleukin-6-promoted cell migration in oral squamous cell carcinoma. <https://doi.org/10.3390/ijms15010545>
- Duicu OM, Pavel IZ, Borcan F, Muntean DM, Cheversean A, Bratu EA, Rusu LC, Karancsi OL (2018) Characterization of the eugenol effects on the bioenergetic profile of SCC-4 human squamous cell carcinoma cell line. <https://doi.org/10.37358/RC.18.9.6577>
- Jinno T, Kawano S, Maruse Y, Matsubara R, Goto Y, Sakamoto T, Hashiguchi Y, Kaneko N, Tanaka H, Kitamura R, Toyoshima T, Jinno A, Moriyama M, Oobu K, Kiyoshim T, Nakamura S (2015) Increased expression of interleukin-6 predicts poor response to chemoradiotherapy and unfavorable prognosis in oral squamous cell carcinoma. <https://doi.org/10.3892/or.2015.3838>
- Geoghegan F, Buckland RJ, Rogers ET, Khalifa K, O'Connor EB, Rooney MF, Behnam-Motlagh P, Nilsson TK, Grankvist K, Porter RK (2017a) Bioenergetics of acquired cisplatin resistant H1299 non-small cell lung cancer and P31 mesothelioma cells. <https://doi.org/10.18632/oncotarget.21885>
- Geoghegan F, Chadderton N, Jane Farrar G, Zisterer DM, Porter RK (2017b) Direct effects of phenformin on metabolism/bioenergetics and viability of SH-SY5Y neuroblastoma cells. <https://doi.org/10.3892/ol.2017.6929>
- Gnaiger E (2020) Mitochondrial pathways and respiratory control. An introduction to OXPHOS analysis. 5th ed. <https://doi.org/10.26124/bec:2020-0002>
- Gu X, Ma Y, Liu Y, Wan Q (2020) Measurement of mitochondrial respiration in adherent cell by Seahorse XF96 Cell Mito Stress Test. <https://doi.org/10.1016/j.xpro.2020.100245>
- Guo J, Su Y, Zhang M (2020) Circ_0000140 restrains the proliferation, metastasis and glycolysis metabolism of oral squamous cell through upregulating CDC73 via sponging miR-182-5p. <https://doi.org/10.1186/s12935-020-01501-7>
- Karavyraki M, Porter RK (2022) Evidence of a role for interleukin-6 in anoikis resistance in oral squamous cell carcinoma. <https://doi.org/10.1007/s12032-022-01664-5>
- Moore SR, Johnson NW, Pierce AM, Wilson DF (2000) The epidemiology of tongue cancer: A review of global incidence. <https://doi.org/10.1111/j.1601-0825.2000.tb00105.x>
- Okura M, Aikawa T, Sawai N, Lida S, Kogo M (2009) Decision analysis and treatment threshold in a management for the N0 neck of the oral cavity carcinoma. <https://doi.org/10.1016/j.oraloncology.2009.03.013>
- O'Neill S, Porter RK, McNamee N, Martinez VG, O'Driscoll L (2019) 2-Deoxy-D-glucose inhibits aggressive triple-negative breast cancer cells by targeting glycolysis and the cancer stem cell phenotype. <https://doi.org/10.1038/s41598-019-39789-9>
- Rheinwald JG, Beckett MA (1981) Tumorigenic keratinocyte lines requiring anchorage and fibroblast support cultures from human squamous cell carcinomas. <https://pubmed.ncbi.nlm.nih.gov/7214336/>

- Schöpf B, Weissensteiner H, Schäfer G, Fazzini F, Charoentong P, Naschberger A, Rupp B, Fendt L, Bukur V, Giese I, Sorn P, Sant'Anna-Silva AC, Iglesias-Gonzalez J, Sahin U, Kronenberg F, Gnaiger E, Klocker H (2020) OXPHOS remodeling in high-grade prostate cancer involves mtDNA mutations and increased succinate oxidation. <https://doi.org/10.1038/s41467-020-15237-5>
- Spinazzi M, Casarin A, Pertegato V, Salviati L, Angelini C (2012) Assessment of mitochondrial respiratory chain enzymatic activities on tissues and cultured cells. <https://doi.org/10.1038/nprot.2012.058>
- Smith PK, Krohn RI, Hermanson GT, Mallia AK, Gartner FH, Provenzano MD, Fujimoto EK, Goeke NM, Olson BJ, Klenk DC (1985) Measurement of protein using bicinchoninic acid. [https://doi.org/10.1016/0003-2697\(85\)90442-7](https://doi.org/10.1016/0003-2697(85)90442-7)
- Srere (1969) Citrate synthase: [EC 4.1.3.7. Citrate oxaloacetate-lyase (CoA-acetylating)] [https://doi.org/10.1016/0076-6879\(69\)13005-0](https://doi.org/10.1016/0076-6879(69)13005-0)
- Tang C-H, Chuang J-Y, Fong Y-C, Maa M-C, Way T-D, Hung C-H (2008) Bone-derived SDF-1 stimulates IL-6 release via CXCR4, ERK and NF- κ B pathways and promotes osteoclastogenesis in human oral cancer cells <https://doi.org/10.1093/carcin/bgn045>
- Warburg O (1956) On the origin of cancer cells. <https://doi.org/10.1126/science.123.3191.309>
- Yellowitz JA, Horowitz AM, Drury TF, Goodman HS (2000) Survey of U.S. dentists' knowledge and opinions about oral pharyngeal cancer. <https://doi.org/10.14219/jada.archive.2000.0239>

Copyright: © 2022 The authors. This is an Open Access preprint (not peer-reviewed) distributed under the terms of the Creative Commons Attribution License, which permits unrestricted use, distribution, and reproduction in any medium, provided the original authors and source are credited. © remains with the authors, who have granted MitoFit Preprints an Open Access publication license in perpetuity.

